Microfluid Nanofluid (2007) 3:723–728
DOI 10.1007/s10404-007-0181-4

SHORT COMMUNICATION

Hydrodynamic dispersion of neutral solutes in nanochannels: the effect of streaming potential

Xiangchun Xuan · David Sinton

Received: 21 February 2007 / Accepted: 23 April 2007 / Published online: 30 May 2007

Abstract An analytical model is developed to account for the effect of streaming potential on the hydrodynamic dispersion of neutral solutes in pressure-driven flow. The pressure-driven flow and the resulting electroosmotic backflow exhibit coupled dispersion effects in nanoscale channels where the hydraulic diameter is on the order of the electrical double layer thickness. An effective diffusion coefficient for this regime is derived. The influence of streaming potential on hydrodynamic dispersion is found to be mainly dependent on an electrokinetic parameter, previously termed the ''figure of merit''. Results indicate that streaming potential decreases the effective diffusion coefficient of the solute, while increasing the dispersion coefficient as traditionally defined. This discrepancy arises from the additional effect of streaming potential on average solute velocity, and discussed herein.

Keywords Hydrodynamic dispersion · Nanochannel · Streaming potential · Neutral solutes · Electroviscous effect

Hydrodynamic dispersion refers to the extension of a locally concentrated solute along the flow direction due to transverse fluid velocity variations. Following the seminal works of Taylor (1953) and Aris (1956), hydrodynamic dispersion has been a topic of interest for over 50 years (Brenner and Edwards 1993). Dispersion in small scale channels has received much attention in the past decade as dispersive effects limit the resolution and throughput of microfluidic lab-on-a-chip devices (Gas and Kenndler 2002; Ghosal 2006). Solute dispersion has been recently studied in pressure-driven (Dutta et al. 2006) and electroosmotic microchannel flows (Ghosal 2004). In nanoscale channels, solute-wall interactions were found to affect both the transport and the hydrodynamic dispersion of charged solutes (Garcia et al. 2005; Pennathur and Santiago 2005a, b; Xuan and Li 2006b; De Leebeeck and Sinton 2006; Griffiths and Nilson 2006). Specifically with respect to ionic dispersion in nanoscale channels, co-ion dispersion was found to be overestimated by theory based on neutral solutes, and counter-ion dispersion underestimated or overestimated depending on relative electrical double layer thickness (De Leebeeck and Sinton 2006).

There is, however, another consequence of the confinement effect in nanochannels, that is the enhancement of flow induced streaming potential (Li 2001). A well established electrokinetic phenomenon (Hunter 1981), streaming potential is an axial potential gradient resulting from the preferential transport of counter-ions in a pressure-driven flow. The resultant electroosmotic back flow, or electroviscous effect (Hunter 1981), was included in a recent paper to determine the solute migration velocity in nanochannels (Xuan and Li 2007). In this communication we examine theoretically the effect of streaming potential on the hydrodynamic dispersion of neutral solutes in nanochannels.

The application of a pressure-driven backflow with an appropriate magnitude has been employed to reduce the hydrodynamic dispersion associated with the electroosmotic flow in, for example, capillary electrophoresis (Datta 1990; Dutta and Leighton 2003; Zholkovskij and

X. Xuan (✉)
Department of Mechanical Engineering,
Clemson University, Clemson, SC 29634-0921, USA
e-mail: xcxuan@clemson.edu

D. Sinton
Department of Mechanical Engineering,
University of Victoria, Victoria, BC, Canada V8W 3P6
e-mail: dsinton@me.uvic.ca

Masliyah 2004). The approach used in these papers will be applied here to first derive a general formula for the dispersion in a combined pressure-driven and electroosmotic flow. Then the streaming potential (and thus the magnitude of electroosmotic backflow) in nanochannels is specified through electrokinetic flow analysis. Finally, a compact formula for the hydrodynamic dispersion is obtained through which the effect of streaming potential is examined quantitatively.

Neutral solutes are advected by the bulk fluid velocity in a slit nanochannel or cylindrical nanotube that may be expressed as

$$u(y) = u_p(y) + u_e(y), \tag{1}$$

where the subscripts p and e denote, respectively, the pressure-driven and electric field-driven velocity components, and y is the transverse coordinate normalized by either the half width of a slit nanochannel or the radius of a cylindrical nanotube. In the former case, the two velocity components are given by (Burgreen and Nakache 1964; Hildreth 1970)

$$u_p(y) = \frac{a^2}{2\mu} P\left(1 - y^2\right), \tag{2}$$

$$u_e(y) = -\frac{\varepsilon\zeta}{\mu} E\left(1 - \frac{\psi(y)}{\zeta}\right), \tag{3}$$

where a is the half width of the slit channel, μ the fluid viscosity, ε the fluid permittivity, ζ the zeta potential of the channel wall, ψ the double-layer potential, P the pressure drop per unit channel length, and E the axial electric field which is internally induced in pressure-driven flow (i.e., streaming potential field). The potential distribution ψ (y) in Eq. 3 is determined from the Poisson–Boltzmann equation, whose solution under the Debye-Huckel approximation is given by (Hunter 1981)

$$\psi(y) = \zeta \frac{\cosh(\phi y)}{\cosh(\phi)}, \tag{4}$$

where $\phi = \kappa a$ is the non-dimensional electrokinetic width with κ being the inverse of Debye length.

The area-averaged velocity $<u>$ may be written in terms of the Poiseuille and electroosmotic components

$$\langle u \rangle = \langle u_p \rangle + \langle u_e \rangle, \tag{5}$$

$$\langle u_p \rangle = \frac{a^2}{3\mu} P, \tag{6}$$

$$\langle u_e \rangle = -\frac{\varepsilon\zeta}{\mu}(1 - \eta) E, \tag{7}$$

$$\eta = \tanh(\phi)/\phi. \tag{8}$$

Hence, the transverse velocity deviation, $\Delta u(y)$ with respect to $<u>$ is expressed as

$$\Delta u(y) = \langle u_p \rangle \left(\frac{1}{2} - \frac{3}{2} y^2\right) + \langle u_e \rangle \left[\frac{\eta}{1-\eta} - \frac{1}{1-\eta}\frac{\cosh(\phi y)}{\cosh(\phi)}\right]. \tag{9}$$

The approach that was used by Datta and Kotamarthi (1990) to study the electrokinetic dispersion in cylindrical capillaries is followed here to obtain an expression for the effective diffusivity $D_{\text{eff}} = D + K$, where D is the molecular diffusivity and K is the hydrodynamic dispersivity defined as

$$K = -\frac{a^2}{D} \int_0^1 \Delta c(y) \Delta u(y) \mathrm{d}y, \tag{10}$$

$$\Delta c(y) = \int_0^y \int_0^{y'} \Delta u(y'') \mathrm{d}y'' \mathrm{d}y'. \tag{11}$$

Substituting Eq. 9 into Eqs. 10 and 11 and then integrating them yield

$$K = \frac{\chi_p a^2}{D} \left[\langle u_p \rangle^2 + \delta_2 \langle u_p \rangle \langle u_e \rangle + \delta_3 \langle u_e \rangle^2\right], \tag{12}$$

$$\chi_p = 2/105, \tag{13}$$

$$\delta_2 = \frac{\eta}{(1-\eta)\chi_p}\left[\frac{2}{15} - \frac{2}{\phi^2} + \frac{6}{\phi^4}\left(\frac{1-\eta}{\eta}\right)\right], \tag{14}$$

$$\delta_3 = \frac{\eta^2}{(1-\eta)^2 \chi_p}\left[\frac{1}{3} + \frac{2}{\phi^2} - \frac{3}{2\eta\phi^2} - \frac{1}{2\eta^2\phi^2\cosh^2(\phi)}\right]. \tag{15}$$

The three terms inside the square brackets in Eq. 12 represent dispersions due to the pressure-driven velocity, the coupling between pressure-driven and electric field-driven flows, and the electroosmotic velocity, respectively. Figure 1 compares the magnitude of δ_2 and δ_3 as a function of electrokinetic width, ϕ. As shown, δ_2 is always larger than δ_3. In the limit of low ϕ (narrowest channel), δ_2 approaches 2 while δ_3 approaches 1, and the square bracketed terms in Eq. 12 reduce to $(< u_p > + < u_e >)^2$ reflecting the similarity of pressure-driven and electroosmotic flow profiles in very narrow nanochannels. In the limit of high ϕ (widest channel), both δ_2 and δ_3 approach zero as the electroosmotic velocity profile becomes essentially plug-like. In that limit, no dispersion-causing velocity gradients are present in the electroosmotic flow component and Eq. 12 reduces to the familiar expression

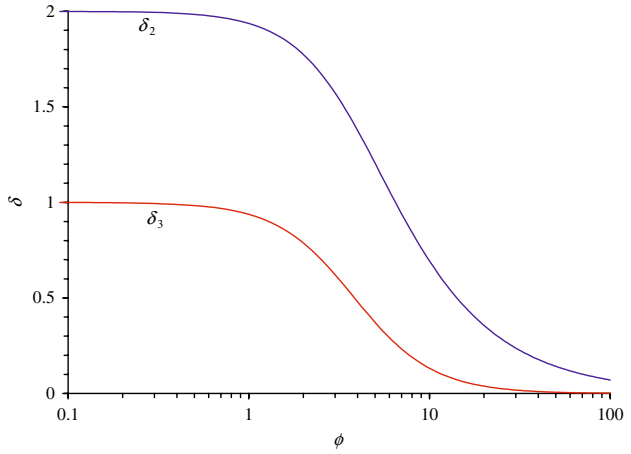

Fig. 1 Illustration of δ_2 and δ_3 as a function of electrokinetic width ϕ

for hydrodynamic dispersion in a pure pressure-driven flow between two parallel plates (Taylor 1953; Aris 1956)

$$K_p = \frac{2a^2\langle u_p\rangle^2}{105D}. \tag{16}$$

Similarily for the case of a pure electroosmotic flow without a pressure-driven flow component, Eq. 12 reduces to an expression identical to that derived by Griffiths and Nilson (1999).

In the case of pressure-driven flow with no externally applied field, downstream accumulation of counter-ions results in the development of a streaming potential, and a corresponding electroosmotic backflow u_e. The electrical current density j for electrokinetic flow in a slit channel is given by (Burgreen and Nakache 1964)

$$j(y) = -\varepsilon\frac{\mathrm{d}^2\psi(y)}{\mathrm{d}y^2}u(y) + \sigma_b\cosh\left[\frac{z_v e\psi(y)}{k_B T}\right]E, \tag{17}$$

where σ_b is the electrical conductivity of the bulk fluid, z_v the valence of electrolyte (assumed symmetric here for simplicity), k_B the Boltzmann's constant, and T the fluid temperature. Since both $\psi(y)$ and $u(y)$ are known, the area-averaged current density J is thus derived as (Xuan and Li 2007)

$$J = -\frac{\varepsilon\zeta}{\mu}(1-\eta)P + \left(\frac{\varepsilon^2\zeta^2}{a^2\mu}F_2 + 2\sigma_b F_3\right)E, \tag{18}$$

$$F_2 = \frac{\phi}{2}\left[\tan h(\phi) - \frac{\phi}{\cosh^2(\phi)}\right] \tag{19}$$

$$F_3 = \frac{1}{2}\int_0^1 \cosh\left[\frac{z_v e\zeta}{k_B T}\frac{\cosh(\phi y)}{\cos h(\phi)}\right]\mathrm{d}y \tag{20}$$

As there is no net current in steady-state pressure-driven flow, i.e., $J = 0$, a streaming potential field, E_{st}, is produced by the applied pressure drop,

$$E_s = \frac{a^2\varepsilon\zeta(1-\eta)}{\varepsilon^2\zeta^2F_2 + 2a^2\sigma_b\mu F_3}P. \tag{21}$$

Note that the function F_3, which is always larger than ½, accounts for the additional contribution of surface conductance to the streaming potential or to the electrical current in Eq. 18 (Hunter 1981; Li 2004; Xuan 2007). Substituting E_{st} into Eq. 7 and referring to Eq. 6 give rise to

$$\frac{\langle u_e\rangle}{\langle u_p\rangle} = -Z, \tag{22}$$

where Z is the previously defined electrokinetic parameter, ''figure of merit'', that governs the efficiency of electrokinetic energy conversion (Morrison and Osterle 1965; Xuan and Li 2006a) and is defined by

$$Z = \frac{3(1-\eta)^2}{F_2 + \beta\phi^2F_3/\zeta^{*2}}, \tag{23}$$

$$\beta = \frac{\lambda_b\mu}{\varepsilon RT}, \tag{24}$$

$$\zeta^* = \frac{z_v e\zeta}{k_B T}, \tag{25}$$

where λ_b is the molar conductivity of the bulk fluid given by σ_b/c_b with c_b being the ionic concentration, and R is the universal gas constant. As Z is unconditionally positive and less than unity, Eq. 22 actually provides a measure of the streaming potential-induced electroosmotic backflow (Li 2001). It is straightforward that Z depends on three non-dimensional parameters: β, ϕ and ζ^*. Specifically, Z is a monotonically decreasing function of the Levine number β that only spans the range of $2 < \beta < 10$ for aqueous solutions (Probstein 1995; Griffiths and Nilson 2005). However, the dependence of Z on both the electrokinetic width ϕ and the zeta potential ζ^* are generally complicated though Z increases with the rise of ζ^* if $\zeta^* < 4$ (Xuan and Li 2006a). For more information about Z, the reader is referred to Xuan and Li (2006a).

Combining Eqs. 12, 16 and 22 provides a measure of the hydrodynamic dispersion in pressure driven flow with the streaming potential effects as compared to that of pressure-driven flow alone

$$K/K_p = 1 - \delta_2 Z + \delta_3 Z^2. \tag{26}$$

As δ_2 is always larger than δ_3 (see Fig. 1) and Z is less than unity (Xuan and Li 2006a), the hydrodynamic dispersion, K, in the presence of streaming potential effects must be less than K_p of a pure pressure-driven flow. It is noted that Eq. 26 also applies to the dispersion in a cylindrical tube with the definition of δ_i provided by Datta and Kotamarthi (1990) and the definition of Z provided by Xuan and Li (2006a).

Hydrodynamic dispersion is expressed in terms of a dispersion coefficient χ in much previous literature (Aris 1956; Dutta et al. 2006; Griffiths and Nilson 2006),

$$K = \chi Pe^2 D, \tag{27}$$

where $Pe = \langle u \rangle a/D$ is the species Peclet number based on the area-averaged species velocity. Following this convention, the dispersion coefficient is $\chi_p = 2/105$ for neutral solutes transported in a pure pressure-driven flow (see Eq. 16). However, to include the effect of streaming potential as presented above, the dispersion coefficient can be expressed as

$$\chi = \frac{2}{105}\frac{1 - \delta_2 Z + \delta_3 Z^2}{(1 - Z)^2}. \tag{28}$$

If the contribution of surface conductance to the streaming potential (see Eq. 21) is ignored, i.e., assuming $F_3 = ½$ in Eq. 23, Z will be overestimated. In that case, the effect of streaming potential on K and χ will both be overestimated. In the limiting case where the streaming potential contribution is negligible, Z approaches zero, $\chi \rightarrow \chi_p$ in Eq. (28), and $K \rightarrow K_p$ in Eq. (26). To quantify the effect of streaming potential (finite Z) on hydrodynamic dispersion, we fix the wall zeta potential to $\zeta = -25$ mV (or $\zeta^* = -0.973$) in compliance with the Debye-Huckel approximation. It is important to note that for a given fluid and channel combination, ζ will, in general, vary with ϕ. One option to address this is to use a surface-charge based potential parameter for scaling instead of zeta potential (De Leebeeck 2006). In this work, and other studies (Griffiths 2006), the zeta potential is used directly, as it may be readily determined through experiment and provides a direct measure of the electroosmotic mobility. All the fluid properties required in the calculation are contained in the Levine number β (Eq. 24). Although the dispersion coefficient χ follows readily from the derivation of dispersivity K, their interpretation requires some care. Hydrodynamic dispersion is characterized first in terms of hydrodynamic dispersivity and then in terms of dispersion coefficient.

Figure 2 shows the hydrodynamic dispersivity ratio K/K_p as a function of electrokinetic width ϕ in both a slit channel (solid lines) and a cylindrical tube (dotted lines) at $\beta = 2$ and 10. As expected, K/K_p is less than 1 in all circumstances indicating that streaming potential effects result in decreased effective solute diffusivity ($D_{eff} = D + K$). The minimum of this ratio appears at about $\phi = 1.7$ for a slit channel and at $\phi = 2.5$ for a circular tube where the figure of merit Z reaches its maximum, and the locations of these minima appear independent of solution properties (as specified through the Levine number β). In these extremes, the streaming potential induced electroosmotic backflow reduces the hydrodynamic dispersion by roughly 25% in a slit channel and more than 20% in a cylindrical tube at $\beta = 2$. The streaming potential effects are more prominent, in general, for lower conductivity and higher viscosity solutions corresponding to low Levine numbers. In both the low and high limits of ϕ, however, K becomes essentially equal to K_p as expected.

Figure 3 shows the dispersion coefficient χ as a function of electrokinetic width ϕ in both a slit channel (solid lines) and a cylindrical tube (dotted lines) at $\beta = 2$ and 10, as labeled. In contrast to the decrease in hydrodynamic dispersivity, K, observed in Fig. 2, Fig. 3 indicates that the dispersion coefficient χ is increased by the effects of streaming potential. Moreover, χ attains a maximum at a relatively larger value of ϕ than that at which K/K_p is minimized. The location of this maxima still appears independent of β. The maximum χ occurs at approximately $\phi = 3.6$ in a slit channel, where the magnitude of the electroosmotic backflow relative to the overall flow, i.e., $\tau = \langle u_e \rangle / (\langle u_e \rangle + \langle u_p \rangle) = Z/(Z-1)$, is –0.105 and –0.021 at $\beta = 2$ and 10, respectively. In a cylindrical tube, the maximum χ occurs at approximately $\phi = 5.3$ while τ remains unvaried at both values of β. There are two noteworthy aspects here: the inverse proportionality between τ and β, and the independence of τ with respect to channel geometry. They might be both due to the linear

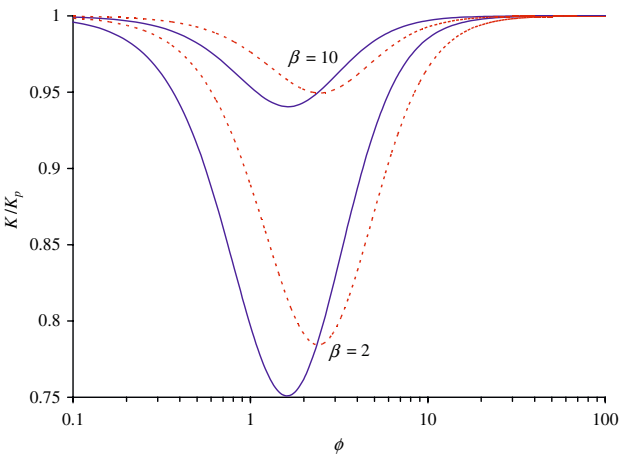

Fig. 2 Plot of the hydrodynamic dispersivity ratio K/K_p in a slit channel (*solid lines*) and a cylindrical tube (*dotted lines*) as a function of electrokinetic width ϕ ($\beta = 2$ and 10 as labeled)

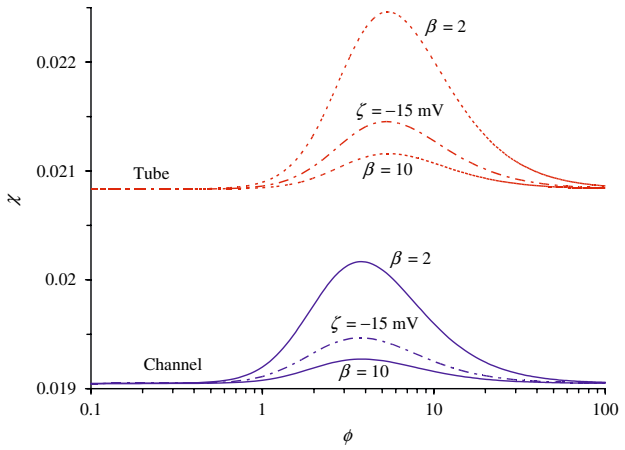

Fig. 3 Plot of the dispersion coefficient χ in a slit channel (*solid lines*) and a cylindrical tube (*dotted lines*) as a function of electrokinetic width ϕ. The *dash-dotted lines* indicate χ at $\beta = 2$ with a zeta potential of $\zeta = -15$ mV instead of –25 mV for the other cases shown. The dissimilar trend in dispersion coefficient plotted here, as compared to the hydrodynamic dispersivity ratio plotted in Fig. 2 are discussed in the text

Debye-Huckel approximation we made in obtaining Eq. 4. Within the range of applicability of this approximation, Fig. 3 also shows χ at $\beta = 2$ with a smaller zeta potential, $\zeta = -15$ mV (dash-dotted lines), compared to –25 mV in all other cases. It is apparent that a higher magnitude of ζ leads to a larger χ throughout the range of ϕ.

The dissimilar trends in hydrodynamic dispersivity and dispersion coefficient observed in Figs. 2, 3, respectively, stem from a dependence of average species velocity on electrokinetic width. As shown in Eq. (27), dispersivity K includes a quadratic dependence on area-averaged solute velocity via the Peclet number. As streaming potential effects increase, electroosmotic backflow velocity increases and the area-averaged solute velocity decreases. Due to coupling of the electroosmotic and pressure-driven flow components, however, the dispersivity does not vary linearly with respect to the solute velocity squared, and the result is the observed variation of dispersion coefficient χ. The net result of these interactions is still a net decrease in dispersivity and a corresponding decrease in effective diffusivity ($D_{\text{eff}} = D + K$) of the solute. Thus despite the common use of dispersion coefficient to describe hydrodynamic dispersion, its interpretation is complicated by an indirect dependence on solute velocity when streaming potential effects are considered. Rather the dispersivity ratio, K/K_p, provides a more clear measure of the effect of streaming potential on hydrodynamic dispersion. It is also important to note that although a neutral solute in a nanoscale channel would exhibit lower effective diffusivity due to streaming potential effects, it would also exhibit a lower average velocity. Thus considering a fixed transport distance in a separation application, the benefit of the lower diffusivity would be partially offset by an increased elution time.

In summary, we have developed an analytical model to examine the effect of streaming potential on the hydrodynamic dispersion of neutral solutes in nanochannels. Compact formulae are derived for the dispersion in terms of normalized zeta potential, ζ^*, non-dimensional electrokinetic width ϕ, and Levine number β. Moreover, these three dimensionless parameters are conveniently combined into the electrokinetic ''figure of merit'' Z that governs the effect of streaming potential on hydrodynamic dispersion. It is found that the streaming potential-induced electroosmotic backflow causes a decrease in dispersivity, and a reduction in the effective diffusion of the solute. These results contrast a corresponding increase in the dispersion coefficient as traditionally defined. This discrepancy arises from the additional effect of streaming potential on average solute velocity, and dispersivity ratio was found to be a more clear measure of the streaming potential effect. The analysis presented here was limited only to small zeta potentials as required by the Debye-Huckel approximation. At higher zeta potentials, the effect of streaming potential on hydrodynamic dispersion in nanochannels is expected to be increased beyond what we have demonstrated in this article.

Acknowledgments The authors are grateful for financial support from Clemson University to X.X. and from the Natural Sciences and Engineering Research Council (NSERC) of Canada to D.S. The authors also thank S. Griffiths for helpful discussions.

References

Aris R (1956) On the dispersion of a solute in a fluid flowing through a tube. Proc R Soc Lond A 235:67–77

Brenner H, Edwards DA (1993) Macrotransport processes. Butterworth-Heinemann, Boston

Burgreen D, Nakache FR (1964) Electrokinetic flow in ultrafine capillary slits. J Phys Chem 68:1084–1091

Datta R (1990) Theoretical analysis of capillary electrophoresis performance. Biotechnol Prog 6:485–493

Datta R, Kotamarthi VR (1990) Electrokinetic dispersion in capillary electrophoresis. AICHE J 36:916–926

De Leebeeck A, Sinton D (2006) Ionic dispersion in nanofluidics. Electrophoresis 27:4999–5008

Dutta D, Leighton DT (2003) Dispersion reduction in open-channel liquid electrochromatographic columns via pressure-driven back flow. Anal Chem 75:3352–3359

Dutta D, Ramachandran A, Leighton DT (2006) Effect of channel geometry on solute dispersion in pressure-driven microfluidic devices. Microfluid Nanofluid 2:275–290

Garcia AL, Ista LK, Petsev DN et al (2005) Electrokinetic molecular separation in nanoscale fluidic channels. Lab Chip 5:1271–1276

Gas B, Kenndler E (2002) Peak broadening in microchip electrophoresis: a discussion of the theoretical background. Electrophoresis 23:3817–3826

Ghosal S (2004) Fluid mechanics of electroosmotic flow and its effect on band broadening in capillary electrophoresis. Electrophoresis 25:214–228

Ghosal S (2006) Electrokinetic flow and dispersion in capillary electrophoresis. Annu Rev Fluid Mech 38:309–338

Griffiths SK, Nilson RH (1999) Hydrodynamic dispersion of a neutral nonreacting solute in electroosmotic flow. Anal Chem 71:5522–5529

Griffiths SK, Nilson RH (2005) The efficiency of electrokinetic pumping at a condition of maximum work. Electrophoresis 26:351–361

Griffiths SK, Nilson RH (2006) Charged species transport, separation, and dispersion in nanoscale channels: autogenous electric field-flow fractionation. Anal Chem 78:8134–8141

Hildreth D (1970) Electrokinetic flow in fine capillary channels. J Phys Chem 74:2006–2015

Hunter RJ (1981) Zeta potential in colloid science, principles and applications. Academic, New York

Li D (2001) Electro-viscous effects on pressure-driven liquid flow in microchannels. Colloid Surf A 191:35–57

Li D (2004) Electrokinetics in microfluidics. Elsevier Academic Press, Burlington

Morrison FA, Osterle JF (1965) Electrokinetic energy conversion in untrafine capillaries. J Chem Phys 43:2111–2115

Pennathur S, Santiago JG (2005a) Electrokinetic transport in nanochannels: 1. Theory. Anal Chem 77:6772–6781

Pennathur S, Santiago JG (2005b) Electrokinetic transport in nanochannels: 2. Experiments. Anal Chem 77:6782–6789

Probstein RF (1995) Physicochemical hydrodynamics. Willey, New York

Taylor GI (1953) Dispersion of soluble matter in solvent flowing slowly through a tube. Prof R Soc Lond A 219:186–203

Xuan X (2007) Revisit of Joule heating in capillary electrophoresis: the contribution of surface conductance. Electrophoresis (in press)

Xuan X, Li D (2006a) Thermodynamic analysis of electrokinetic energy conversion. J Power Sources 156:677–684

Xuan X, Li D (2006b) Electrokinetic transport of charged solutes in micro- and nanochannels, the influence of transverse electromigration. Electrophoresis 27:5020–5031

Xuan X, Li D (2007) Solute separation in nanofluidic channels, pressure-driven or electric field-driven. Electrophoresis 28:627–634

Zholkovskij EK, Masliyah JH (2004) Hydrodynamic dispersion due to combined pressure-driven and electroosmotic flow through microchannels with a thin double layer. Anal Chem 76:2708–2718